Analysis of mesoscopic loss effects in fine layered fluid-saturated poroelastic sediments

UNLP, 11 Octubre de 2012

Anisotropic poroelasticity and mesoscopic loss. I

- Reservoirs rocks consists usually of thinly layered fluid-saturated poroelastic sediments.
- The traveling P-waves induce fluid-pressure gradients at mesoscopic-scale heterogeneities, generating interlayer fluid flow and slow (diffusion) Biot waves (mesoscopic loss mechanism).
- These finely layered sediments behave like viscoelastic transversely isotropic (VTI) media at long wavelengths.

Anisotropic poroelasticity and mesoscopic loss. II

- For fluid-saturated poroelastic media (Biot's media), White et al. (1975) were the first to introduce the mesoscopic-loss mechanism in the framework of Biot's theory.
- Gelinsky and Shapiro (GPY, **62**, 1997) obtained the relaxed and unrelaxed stiffnesses of the equivalent poro-viscoelastic medium to a finely layered horizontally homogeneous (FLHH) Biot's medium.
- For a FLHH Biot's medium, Krzikalla and Müller (GPY, **76**, 2011) combined the two previous models to obtain the five complex and frequency-dependent stiffnesses of the equivalent VTI medium.

Anisotropic poroelasticity and mesoscopic loss. III

- Krzikalla and Müller assumed fluid-flow direction perpendicular to the layering plane. Hence, the model uses only one relaxation function, associated with the symmetry-axis P-wave stiffness.
- To test the model and provide a more general modeling tool, we present a numerical upscaling procedure to obtain the complex stiffnesses of the effective VTI medium.
- The method uses the Finite Element Method (FEM) to solve Biot's equation of motion in the space-frequency domain with boundary conditions representing compressibility and shear harmonic experiments.

TIV media and fine layering. I

Let us consider isotropic fluid-saturated poroelastic layers.

$\mathbf{u}^s(\mathbf{x}), \mathbf{u}^f(\mathbf{x})$: time Fourier transform of the displacement vector of the solid and fluid relative to the solid frame, respectively.

$\mathbf{u} = (\mathbf{u}^s, \mathbf{u}^f)$

$\sigma_{kl}(u), \mathbf{p}_f(u)$: Fourier transform of the total stress and the fluid pressure, respectively

On each plane layer n in a sequence of N layers, the **frequency-domain stress-strain relations** are

$$\sigma_{kl}(u) = 2\mu\,\varepsilon_{kl}(u^s) + \delta_{kl}\left(\lambda_{_G}\,\nabla\cdot u^s + \alpha M \nabla\cdot u^f\right),$$
$$\mathbf{p}_f(u) = -\alpha M \nabla\cdot u^s - M\nabla\cdot u^f.$$

TIV media and fine layering. II

Biot's equations of motion:

$$-\omega^2 \rho u^s(x,\omega) - \omega^2 \rho_f u^f(x,\omega) - \nabla \cdot \sigma(u) = 0,$$
$$-\omega^2 \rho u^f(x,\omega) - \omega^2\, m\, u^f(x,\omega) + \mathrm{i}\omega \frac{\eta}{\kappa} u^f(x,\omega) + \nabla p_f(u) = 0,$$

$\omega = 2\pi f$: **angular frequency**

$m = \frac{\mathcal{T}\rho_f}{\phi}$: **mass coupling coefficient** $\mathcal{T}$:**tortuosity factor**

$\rho = (1-\phi)\rho_s + \phi\rho_f$,

ρ_s **and** ρ_f: **mass densities of the solid grains and fluid, respectively**

η: **fluid viscosity** κ: **frame permeability**

TIV media and fine layering. III

τ_{ij}: **stress tensor of the equivalent VTI medium**

Assuming a closed system($\nabla \cdot u^f = 0$**), the corresponding stress-strain relations, stated in the space-frequency domain, are**

$$\tau_{11}(u) = p_{11}\,\epsilon_{11}(u^s) + p_{12}\,\epsilon_{22}(u^s) + p_{13}\,\epsilon_{33}(u^s),$$
$$\tau_{22}(u) = p_{12}\,\epsilon_{11}(u^s) + p_{11}\,\epsilon_{22}(u^s) + p_{13}\,\epsilon_{33}(u^s),$$
$$\tau_{33}(u) = p_{13}\,\epsilon_{11}(u^s) + p_{13}\,\epsilon_{22}(u^s) + p_{33}\,\epsilon_{33}(u^s),$$
$$\tau_{23}(u) = 2\,p_{55}\,\epsilon_{23}(u^s),$$
$$\tau_{13}(u) = 2\,p_{55}\,\epsilon_{13}(u^s),$$
$$\tau_{12}(u) = 2\,p_{66}\,\epsilon_{12}(u^s).$$

This approach provides the complex velocities of the fast modes and takes into account interlayer flow effects.

TIV media and fine layering. IV

Krzikalla and Müller (GPY, 76, 2011) proposed a model to determine the stifnees p_{IJ} for a stack of two thin alternating porous layers.

These analytical p_{IJ}'s will be used to check the results of the FEM to be used next to determine these coefficients.

Using the p_{IJ}'s and the thickness weighted average of the bulk density will in turn allow us to determine the phase velocity and quality factors for the qP, qS and SH waves.

The harmonic experiments to determine the stiffness coefficients. I

To determine the complex stiffness p_{IJ}'s we solve Biot's equation in the 2D case on a reference square $\Omega = (0, L)^2$ with boundary Γ in the (x_1, x_3)-plane, with boundary conditions representing harmonic compressibility and shear tests, as explained for the fractured viscoelastic case.

Over the seismic band of frequencies, the acceleration (ω^2) terms are negligible relative to the viscous resistance and can be discarded, so that we solve the diffusion Biot's equation.

Schematic representation of the harmonic compressibility and shear tests in Ω

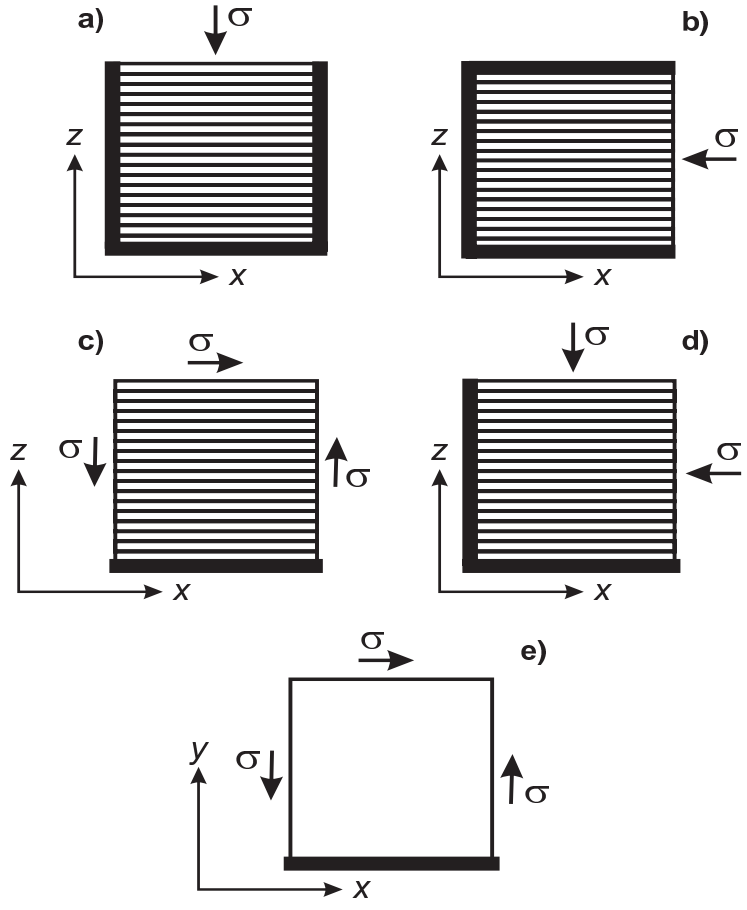

Examples. I

- The methodology is applied to the Utsira aquifer of the North Sea, where CO_2 has been injected during the last 15 years.
- The example considers a sequence of gas-saturated sandstone and mudstone layers, representing models of the reservoir and cap rock of the aquifer system.
- The quality factors and velocities as a function of frequency and propagation angle are tested against those provided by the theory for laterally homogeneous layers.
- Examples for highly heterogeneous Biot's media are also presented.

Examples. II

Let us consider the North-Sea Utsira formation located 800 m below the sea bottom, which contains a highly permeable sandstone, where carbon dioxide (CO_2) has been injected in the Sleipner field.

Within the Utsira aquifer, compacted mudstone layers have been identified, acting as barriers to the upward migration of the CO_2.

Examples. III

Properties of the Utsira formation.

	Sandstone	Mudstone
Grain bulk modulus, K_s (GPa)	40	20
density, ρ_s (kg/m^3)	2600	2600
Frame bulk modulus, K_m (GPa)	1.37	7
shear modulus, μ_m (GPa)	0.82	6
porosity, ϕ	0.36	0.2
permeability, κ (D)	1.6	0.01
Brine density, ρ_w (kg/m^3)	1030	1030
viscosity, η_w (Pa s)	0.0012	0.0012
bulk modulus, K_w (GPa)	2.6	2.6
CO_2 density, ρ_g (kg/m^3)	505	–
viscosity, η_g (Pa s)	0.00015	–
bulk modulus, K_g (MPa)	25	–

Examples. IV

The upper part of the aquifer (cap rock) is the location where the proportion of mudstone may be substantial.

The example considers alternating layers of brine-saturated mudstone and CO_2-saturated sandstone of thicknesses 5 cm and 1 cm, respectively, and a period of 6 cm.

It models the case in which the original brine has been replaced by CO_2 and the sequence may represent possible leakages to the cap rock.

The figures compares the analytical p_{IJ} with the FE solution for several periods of the stratification.

P-wave phase velocities perpendicular (Vp33) and parallel (Vp11) to the layering plane

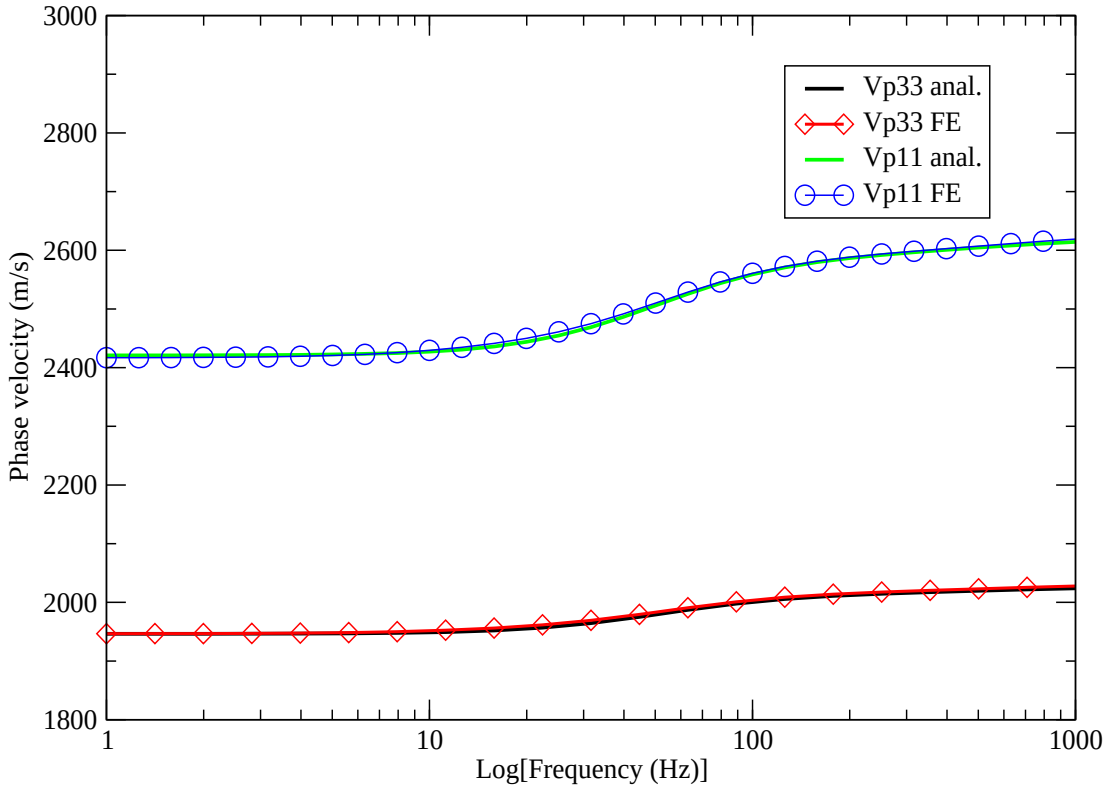

The medium is a sequence of brine-saturated mudstone and CO_2-saturated sandstone layers with thicknesses of 5 cm and 1 cm, respectively. Symbols indicate FE values.

Dissipation factors perpendicular (1000/Q33) and parallel (1000/Q11) to the layering plane

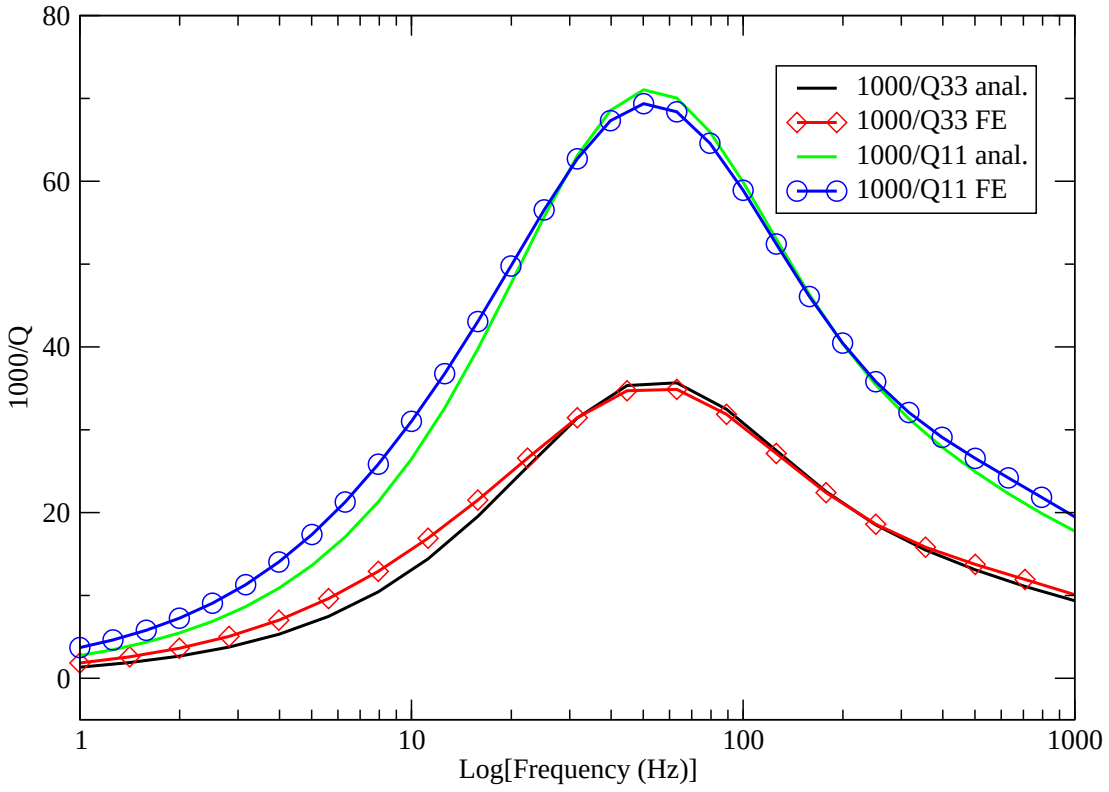

The medium is a sequence of brine-saturated mudstone and CO_2-saturated sandstone layers with thicknesses of 5 cm and 1 cm, respectively. Symbols indicate FE values.

Phase velocities at 50 Hz as function of the propagation angle

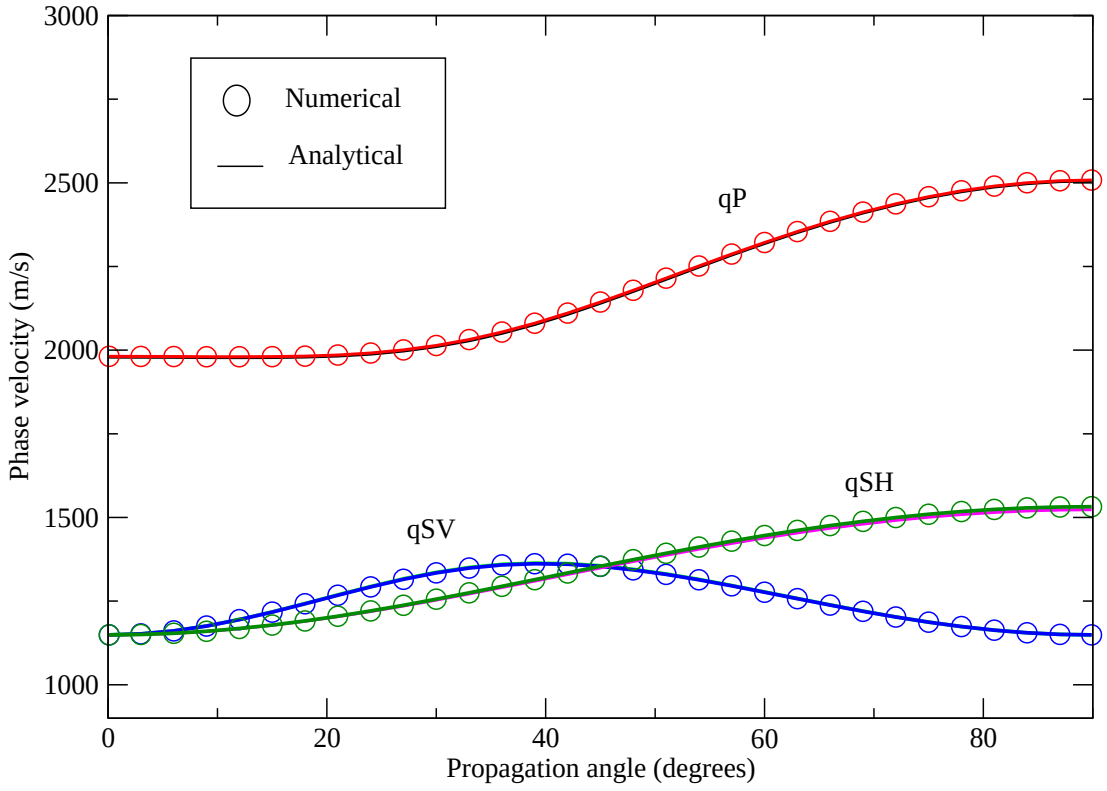

The medium is a sequence of mudstone and CO_2-saturated sandstone layers with thicknesses of 5 cm and 1 cm, respectively

Dissipation factors at 50 Hz as function of the propagation angle

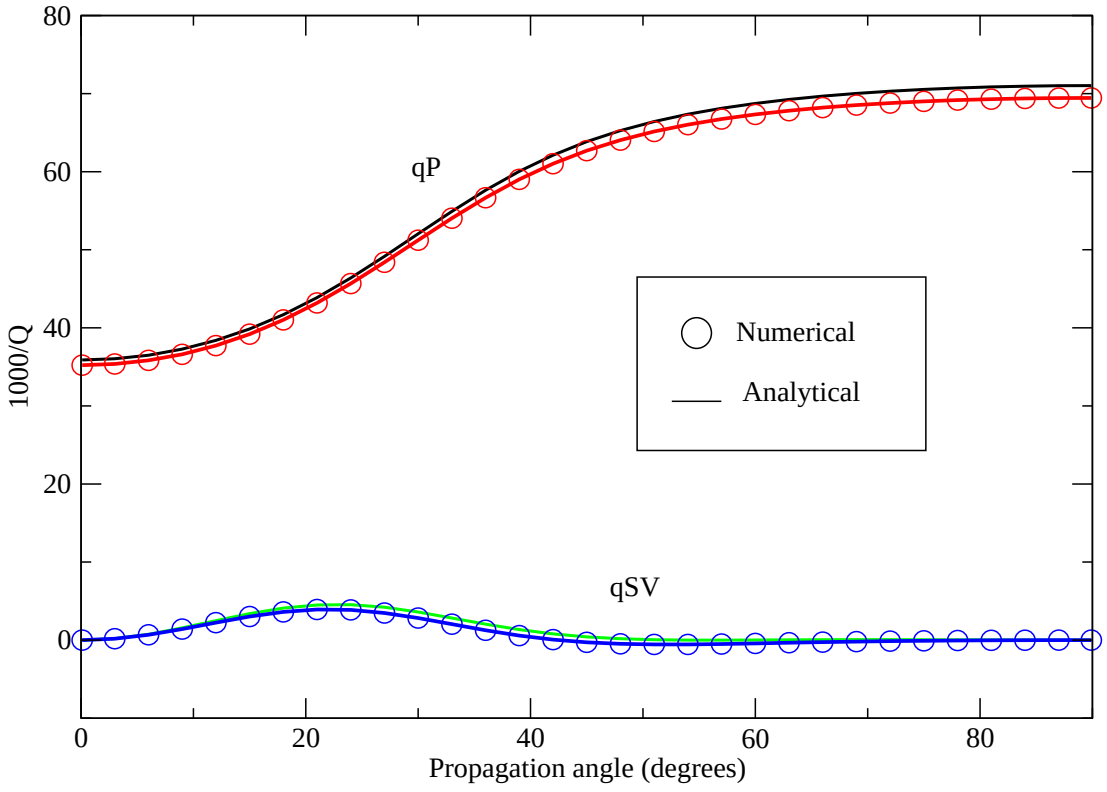

The medium is a sequence of mudstone and CO_2-saturated sandstone layers with thicknesses of 5 cm and 1 cm, respectively

PATCHY SATURATION. CO_2-BRINE DISTRIBUTION

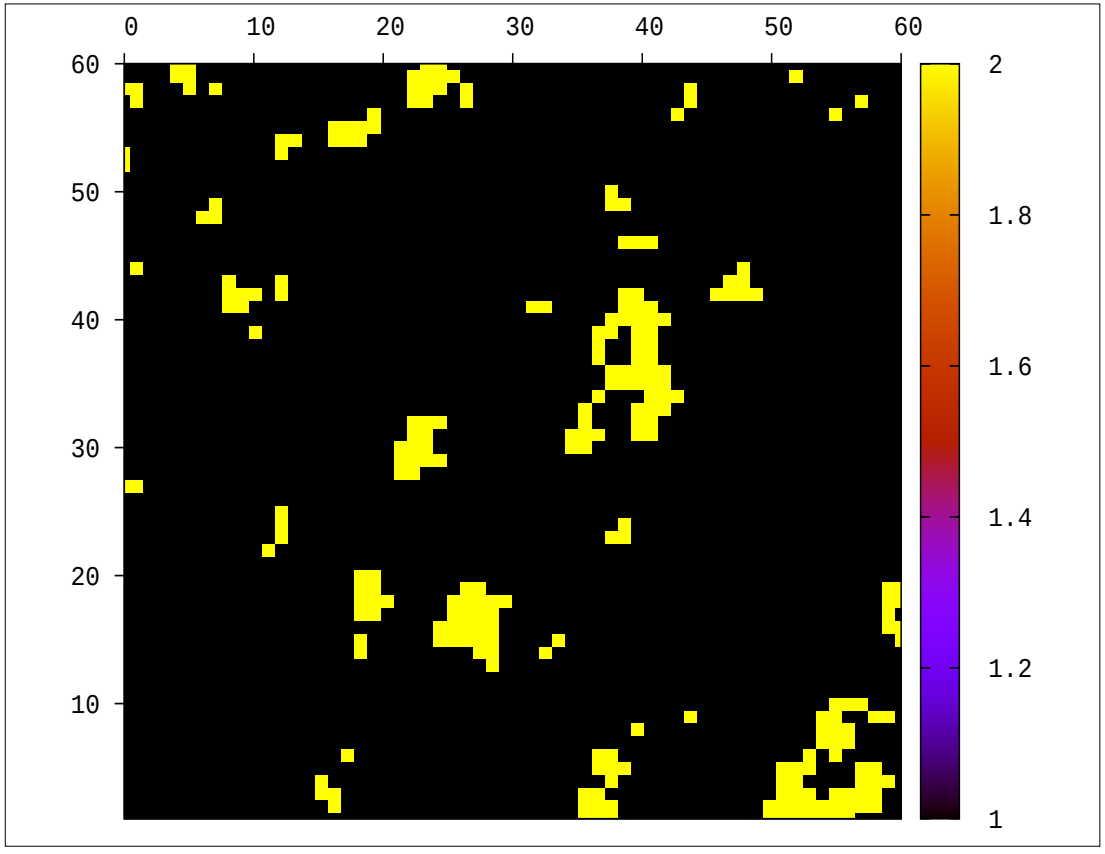

Yellow zones correspond to CO_2 saturation and the black ones to pure brine saturation. The overall CO_2 saturation is 7 percent.

PATCHY SATURATION. Coefficient λ_G (Pa)

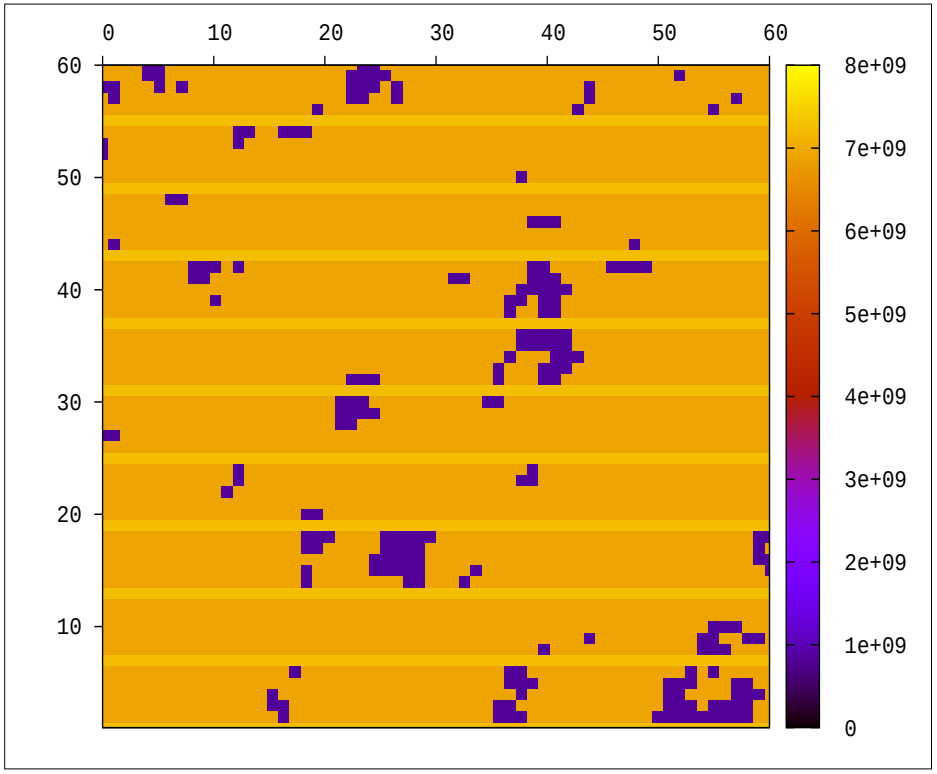

PATCHY SATURATION. P-wave phase velocities parallel (Vp11) to the layering plane.

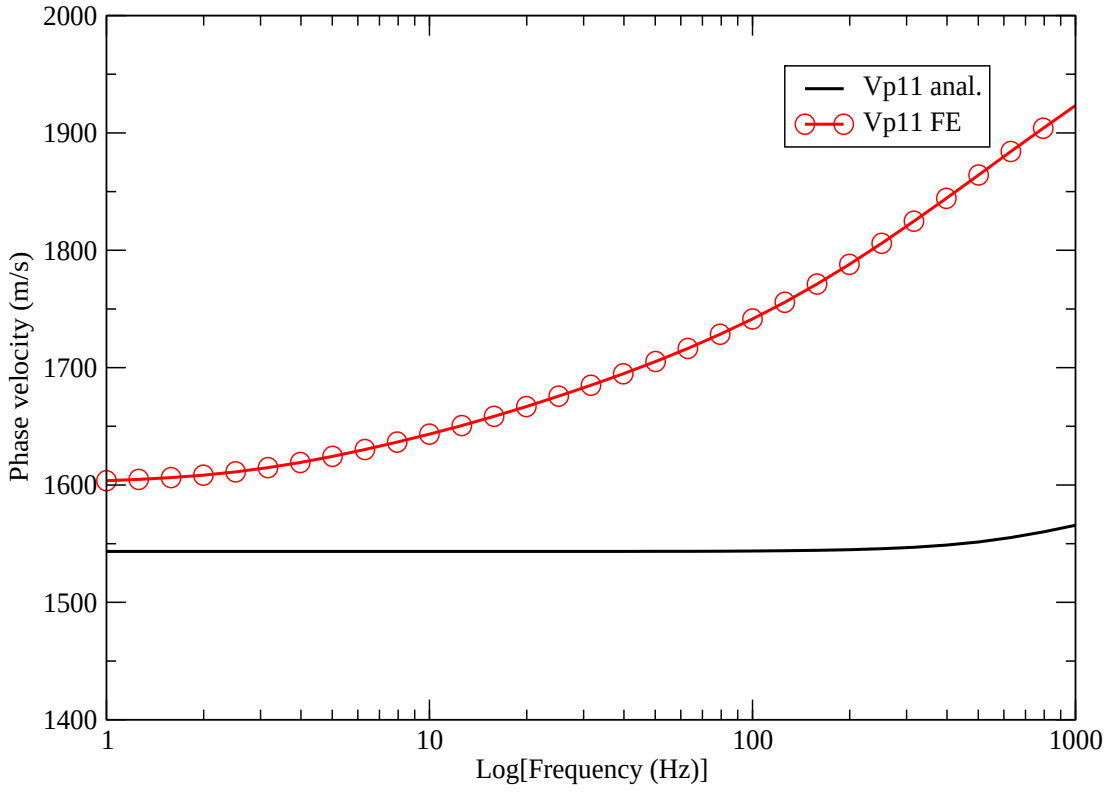

Sequence of 5 cm patchy-saturated Utsira and 1 cm brine-saturated mud . The Analytical curve corresponds to the same sequence but for CO_2-saturated Utsira.

PATCHY SATURATION. Dissipation factors parallel (1000/Q11) to the layering plane.

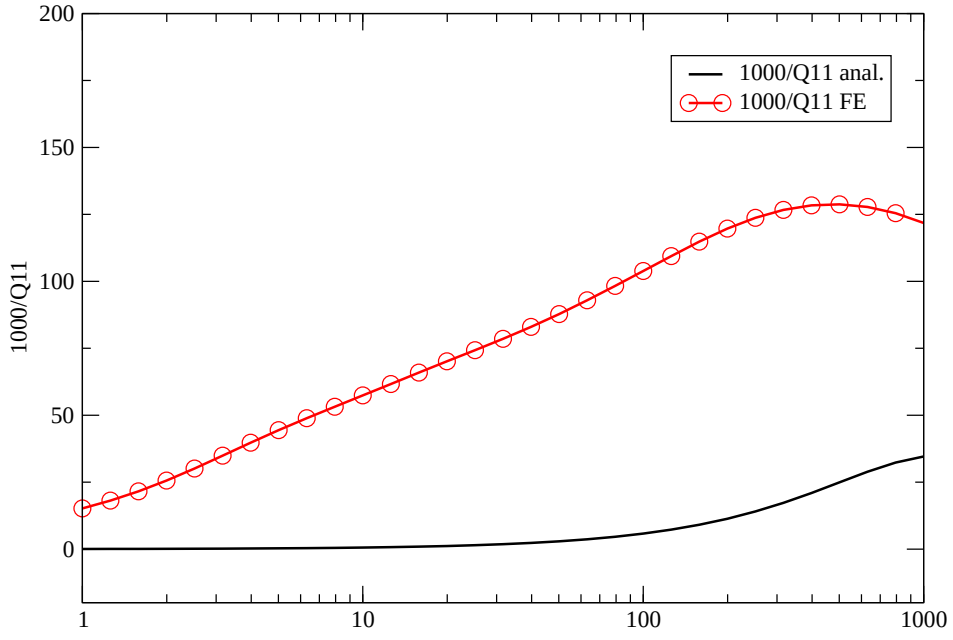

Sequence of 5 cm patchy-saturated Utsira and 1 cm brine-saturated mud . The Analytical curve corresponds to the same sequence but for CO_2-saturated Utsira.

PATCHY SATURATION. P-wave phase velocities perpendicular (Vp33) to the layering plane.

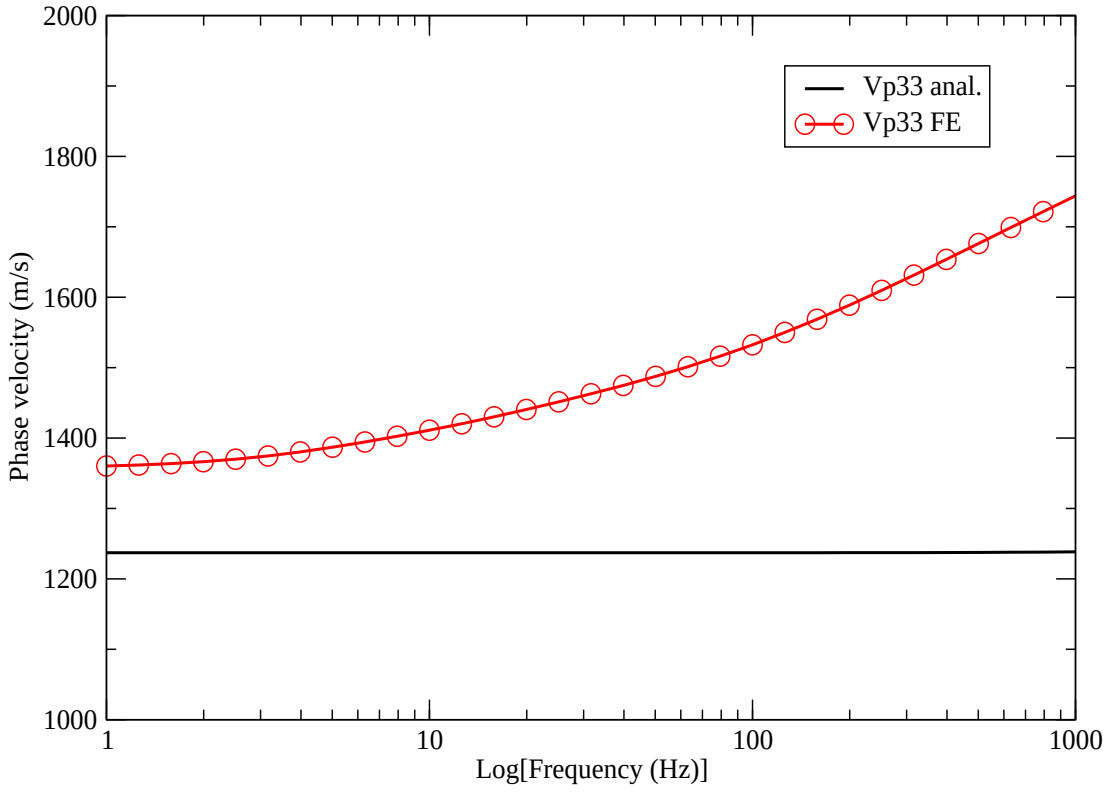

Sequence of 5 cm patchy-saturated Utsira and 1 cm brine-saturated mud . The Analytical curve corresponds to the same sequence but for CO_2-saturated Utsira.

PATCHY SATURATION. Dissipation factors perpendicular (1000/Q33) to the layering plane.

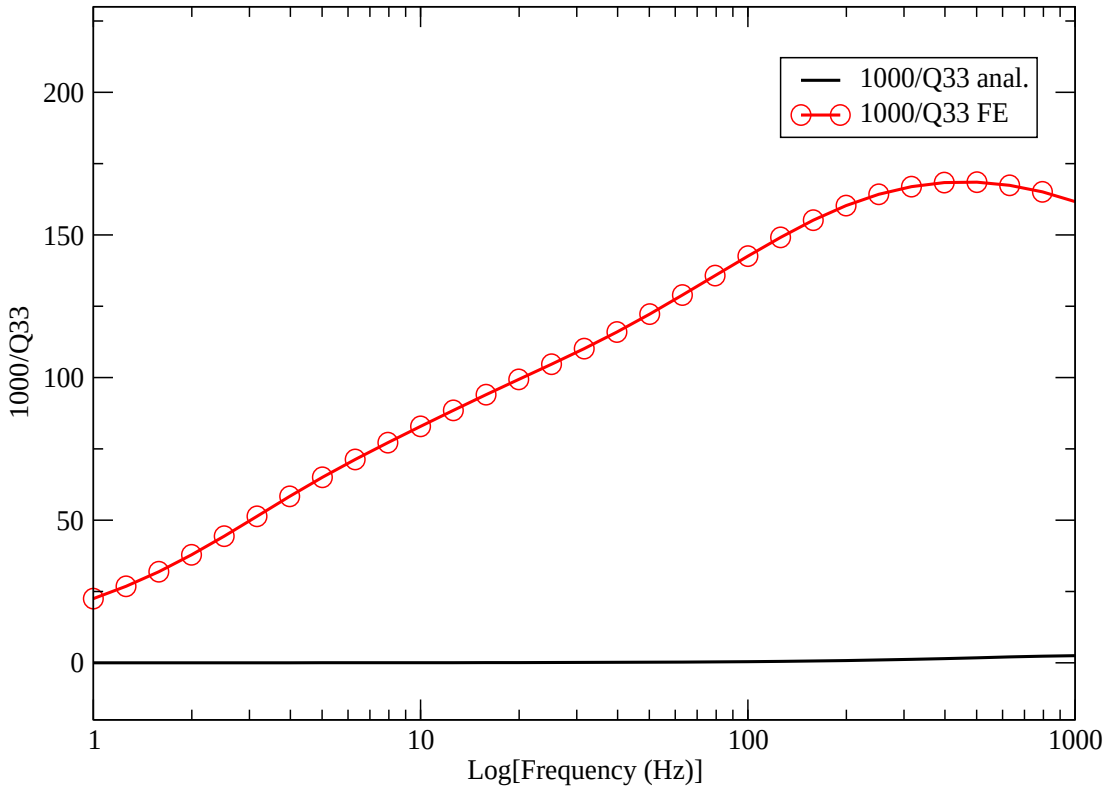

Sequence of 5 cm patchy-saturated Utsira and 1 cm brine-saturated mud . The Analytical curve corresponds to the same sequence but for CO_2-saturated Utsira.

CONCLUSIONS. I

- We presented a novel numerical FEM to obtain the complex and frequency-dependent stiffnesses of a VTI homogeneous medium equivalent to a finely layered Biot's medium.
- The methodology is based on the FE solution Biot's equation in the space-frequency domain to simulate harmonic compressibility and shear tests.
- The FE results were checked againts a theory valid for laterally homogeneous layers and 1D-fluid-flow direction.

CONCLUSIONS. II

- Velocity and attenuation anisotropy can be observed in the qP and qSV wave modes, with attenuation higher along the layering plane for the case being analyzed.
- SV-Shear attenuation is much weaker than the qP attenuation, and SH waves are lossless.
- The FEM was applied to determine a VTI homogeneous medium equivalent to a finely layered patchy-saturated Biot's medium.

FUTURE WORK

- fractures in fluid-saturated porous rocks (Schoemberg et al. theories)
- Effective media for fractured fluid-saturated porous rocks.
- Wave propagation in fluid-saturated porous rocks with fractures at the macroscale using effective media theories.